Anti-angiogenic activity of uncoated- and*N,O*-carboxymethyl-chitosan surface modified-Gelucire®50/13 based solid lipid nanoparticles for oral delivery of curcumin

Sara Perteghella[a], Delia Mandracchia[b,1], Maria Luisa Torre[a], Roberto Tamma[c], Domenico Ribatti[c], Adriana Trapani[b,*], Giuseppe Tripodo[a]

[a] *Department of Drug Sciences, University of Pavia, viale Taramelli, 12, 27100, Pavia, Italy*

[b] *Department of Pharmacy-Drug Sciences, University of Bari"Aldo Moro", via Orabona, 4, 70125, Bari, Italy*

[c] *Department of Basic Medical Sciences, Neurosciences, and Sensory Organs, University of Bari Medical School, Piazza Giulio Cesare 11, 70100, Bari, Italy*

A B S T R A C T

The co-administration of anti-tumor and anti-angiogenesis agents represents a well-established strategy for cancer treatment. However, the clinical use of this"combined therapy"approach showed several limitations probably due to the inability of most angiogenic inhibitors to target tumor vessels. Herein, we evaluated the *in vitro*angiogenesis e ✓ ects of*N,O*-carboxymethyl chitosan (*N,O*-CMCS) surface modi ⌕ed curcumin (CUR)-loaded solid lipid nanoparticles (SLN) intended for CUR oral administration. For this purpose, SLN formulations based on Gelucire®50/13 were prepared and characterized for their physicochemical properties. From stability tests such SLN resulted useful to protect CUR from oxidative and hydrolytic degradation for a long period at 4 °C. Moreover,*N,O*-CMCS-*c*-CUR SLN (F4) displayed enhanced cytocompatibility with Caco-2 cells. Data from angiogenesis studies showed that the CUR-unloaded and surface unmodi ⌕ed SLN (b-SLN, F1) possess anti-angiogenic activity and, moreover, due to the features of the coating polysaccharide, F4 may constitute an anti-angiogenic delivery platform for CUR oral delivery and such delivery system seems promising in vascular angiogenesis inhibition.

1. Introduction

Despite notable advances made in the treatment of cancer, it still constitutes one of leading causes of death, particularly in more developed regions [1]. A very crucial process in determining proliferation and growth of solid tumors is represented by the angiogenesis consisting in the formation of new blood vessels which are necessary to provide oxygen and nutrients and to remove metabolic waste in tumor tissues [2–4]. Several factors are involved in the formation of new blood vessels and an appropriate balance should occur between compounds endowed with pro-angiogenic activity [*e.g.*, vascular endothelial growth factor (VEGF), basic ⌕broblast growth factor (bFGF) and transforming growth factor-⌕(TGF-⌕)] and those with anti-angiogenesis one (*e.g.*, angiostatin and endostatin) [4]. Therefore, the co-administration of anti-tumor agents and anti-VEGF monoclonal antibodies represents a well-established strategy for cancer treatment. However, despite some advantages were noted using this"combined therapy"approach, the clinical use of the anti-angiogenic therapeutic strategy showed several limitations such as toxicity and acquired drug resistance [5]. It has been mainly attributed to the inability of most angiogenesis inhibitors to target tumor vessels due to unsatisfactory biodistribution [5]. To increase the e cacy of the"anti-tumor/anti-angiogenesis agent"combined strategy the use of nanocarriers has been proposed [6]. It because nanosized carriers show several advantages including the ability of delivering large amounts of drugs and they may favour tumor targeting. Moreover, nanocarriers are able to overcome

*Abbreviations:*bFGF, basic ⌕broblast growth factor; CAM, embryo chorioallantoic membrane; CUR, Curcumin; F1, blank-SLN, surface unmodi ⌕ed and curcumin free SLN; F2, CUR-SLN, surface unmodi ⌕ed and CUR-loaded SLN; F3,*N,O*-CMCS-*c*-SLN,*N,O*-CMCS-decorated- and curcumin-unloaded SLN; F4,*N,O*-CMCS-*c*-CUR-SLN,*N,O*-CMCS-decorated- and curcumin-loaded SLN; fetal bovine serum FBS, fetal bovine serum;*N*-CMCS,*N*-carboxymethyl chitosan;*N,O*-CMCS,*N,O*-carboxymethyl chitosan; SGF, Simulated gastric uid; SIF, Simulated intestinal uid; SLN, Solid lipid nanoparticles; TGF-⌕, transforming growth factor-⌕; VEGF, vascular endothelial growth factor

* Corresponding author. Dept. of Pharmacy-Drug Sciences, University of Bari"Aldo Moro", 70125, Bari, Italy.
E-mail address: adriana.trapani@uniba.it (A. Trapani).

[1] Present address: Department of Molecular and Translational Medicine, University of Brescia, Viale Europa 11, Brescia, 25123, Italy.

further limitations of conventional formulations including, unsatisfactory biodistribution and development of multidrug-resistance (MDR) frequently occurring in cancer cells [5,6]. Thus, a number of polymeric nanoparticles based on different polymers such as*N*-(2-hydroxypropyl)methacrylamide (HPMA), poly(lactic co-glycolic acid) (PLGA), poly(alkyl cyanoacrylate) (PACA), poly-(L-lactic) (PLLA) and polysaccharides (*e.g.*, chitosan and its derivatives) have been employed for angiogenesis inhibition therapy [5,7–9]. Amphiphilic polymers, including poly(ϵ-caprolactone)-polyethyleneglycol (PCL-PEG) and carboxymethyl chitosan-PCL (CMCS-PCL), which could self-assemble into polymeric micelles in aqueous solution have also been used for the same purpose [5,10–12]. Among lipid-based nanocarriers, liposomes have been widely used for anti-angiogenic activity but they suffer from some limitations such as low drug loading and, therefore, alternative lipid based formulations are welcome [13]. In this context, solid lipid nanoparticles (SLN) can be valuable candidates for anti-angiogenic therapy since they are characterized by several advantages including enhanced safety and stability, controlled drug release, and can be applied for both hydrophobic and hydrophilic drugs [14,15]. Moreover, SLN may be employed following several administration routes including the most convenient for patients,*i.e.,*the oral one [16–18]. However, to the best our knowledge, there is only one example in literature of anti-angiogenic therapy based on SLN encapsulating an angiogenesis inhibitor agent [19].

Recently, it has been reported that*N*-carboxymethyl chitosan (*N*-CMCS) coated curcumin (CUR)-loaded SLN showed increased cytotoxicity and cellular uptake by MCF-7 cells as well as enhanced lymphatic uptake and oral bioavailability [20]. CUR is a hydrophobic drug characterized by low aqueous solubility and poor absorption and several formulation approaches have been employed to overcome such unfavourable features of hydrophobic drugs including the use of liposomes [21], cyclodextrins [22,23] and polymeric micelles [21]. CUR is also endowed with potent anti-angiogenesis activity and, combined with doxorubicin, showed remarkable enhancement of anti-cancer activity [24,25]. On the other hand, it has also been recently demonstrated that*N,O*-carboxymethyl chitosan (*N,O*-CMCS) showed relevant anti-tumor activity by inhibition of angiogenesis and stimulation of immune functions [26]. Based on this background, it seemed of interest to investigate the angiogenesis effects of*N,O*-CMCS surface modified CUR-loaded SLN intended for oral administration. In this approach, our working hypothesis was that the polysaccharide*N,O*-CMCS decorating SLN may give anti-angiogenic features to the whole delivery system and, therefore, could be effective in anti-cancer therapy. To test this hypothesis, in this paper the preparation of CUR-loaded SLN based on Gelucire®50/13 as lipid matrix and their surface modification with *N,O*-CMCS is described. Gelucire®50/13 was selected considering that it is constituted by PEG-esters (Stearoyl polyoxyl-32 glycerides), a small glyceride fraction and free PEG and may self-emulsify on contact with aqueous media. Moreover, to evaluate a possible application of such surface modified SLN as oral drug delivery systems, their physical stability in simulated gastro-intestinal fluids as well as cytotoxicity, uptake and transport studies through Caco-2 cells were also investigated [27]. Finally, the anti-angiogenic activity of these lipid nanocarriers, was evaluated by the*in vivo*chick embryo chorioallantoic membrane assay [24,28,29].

2. Materials and methods

2.1. Materials

Gelucire®50/13 was a gift by Gattefossè (Milan, Italy). Curcumin (CUR), Tween®85 and Tween®80 were purchased by Sigma Aldrich (Milan, Italy).*N,O*-CMCS (deacetylation degree 92.8%), was purchased from Heppe Medical Chitosan GmbH [Halle (Saale), Germany] and, according to manufacturer instructions, possesses a molecular weight in the range of 30–500 kDa (GPC). Dialysis bags (cut-off 3500 Da) were provided by SpectraPore (Italy). Caco-2 cells (CACO-2 Passage 43) were purchased from the European Collection of Authenticated Cell Cultures Cell Bank (ECACC, Salisbury, UK). All reagents used for cell cultures were obtained from Euroclone (Milan, Italy).

2.2. Preparation of unmodified-as well as N,O-CMCS surface modified SLN with and without curcumin

The melt-emulsification method was followed to prepare the SLN studied in this work [30–32]. Besides the blank-SLN(*i.e.*, b-SLN, F1), the surface unmodified and CUR-loaded SLN (CUR-SLN, F2), the*N,O*-CMCS-coated- and CUR-unloaded SLN (*N,O*-CMCS-*c*-SLN, F3) and the *N,O*-CMCS-coated- and CUR-loaded SLN (*N,O*-CMCS-*c*-CUR-SLN, F4) were prepared.

*Preparation of b-SLN (F1).*After melting 60 mg of Gelucire®50/13 at 70 °C, in a separate vial an aqueous solution (1.37 mL of water) containing the surfactant (Tween®85, 60 mg) was used and it was heated at 70 °C. The resulting mixture was added to the melted phase at 70 °C in order to obtain an emulsion by homogenization at 12300 rpm for 2 min with an UltraTurrax model T25 apparatus (Janke and Kunkel, Germany). Afterwards, the nanosuspension was cooled at room temperature and the resulting SLN centrifuged (16,000×*g*, 45 min, Eppendorf 5415D, Germany).

*Preparation of CUR-SLN (F2).*The previously described procedure for F1 preparation was followed but 6 mg of CUR were added to the melted lipid prior to pour the aqueous phase.

*Preparation of N,O-CMCS-c-SLN (F3).*To allow the SLN surface modification of F1, 0.5 mL of the resulting nanosuspension were incubated with 1 mL of a*N,*O-CMCS aqueous solution (3 mg/mL) at room temperature for 3 h. At the end of the incubation time, centrifugation was performed as above mentioned (16,000×*g*, 45 min, Eppendorf 5415D, Germany).

*Preparation of N,O-CMCS-c-CUR-SLN (F4).*After the Ultraturrax treatment employed in F2 preparation, 0.5 mL of the fluorescent nanosuspension were surface modified with 1 mL of a*N,*O-CMCS aqueous solution (3 mg/mL) upon incubation at room temperature for 3 h under light protection. After incubation, centrifugation step was performed (16,000×*g*, 45 min, Eppendorf 5415D, Germany).

2.3. Physicochemical characterization of SLN

2.3.1. Particle size, zeta potential and TEM visualization

To gain information on the physicochemical characteristics of the nanosystems prepared, particle size and polydispersity index (PDI) of SLN were determined by using a ZetasizerNanoZS (ZEN 3600, Malvern, UK) apparatus according to photon correlation spectroscopy (PCS) mode. In the cuvette, each sample was diluted 1:1 (v:v) with double distilled water. The determination of the zeta-potential was performed using laser Doppler anemometry (ZetasizerNanoZS, ZEN 3600, Malvern, UK) after dilution of the sample 1:20 (v:v) in the presence of KCl (1 mM, pH 7) [33,34]. The morphology of SLN was studied by TEM analysis. To this end, the samples were processed by dropping 10μL of a 1 mg/mL suspension of the sample on a copper grid. The so prepared grid was dried at 25 °C in a desiccator and subsequently stained with uranyl acetate. TEM analysis was performed by a Jeol-Jem-1200EXII instrument, Japan.

2.3.2. Solid state studies

To gain information on the solid state of SLN prepared, the corresponding FT-IR spectra and DSC thermograms were recorded. The FT-IR spectroscopy analyses were performed on SLN using a PerkinElmer 1600 FT-IR spectrometer (PerkinElmer, Italy). To acquire FTIR spectra all samples were mixed with an appropriate amount of KBr. The range examined was 4,000–400 cm^{-1} with a resolution of 1 cm^{-1}.

DSC thermograms were performed using a Mettler Toledo DSC 822e STARe 202 System equipped with a DSC MettlerSTARe Software. For

DSC analysis, aliquots of about 5 mg of each product were placed in an aluminium pan and hermetically sealed. The scanning rate was of 5 °C/min under a nitrogen flow of 20 cm^3/min and the temperature range was from 25 to 275 °C. The calorimetric system was calibrated in transition temperature by using indium (purity 99.9%) and following the procedure of the MettlerSTARe Software. Each experiment was carried out in triplicate to check the reproducibility.

2.3.3. Determination of encapsulation efficiency and loading capacity

To determine the amount of CUR loaded in the SLN, the encapsulation efficiency (E.E.) was calculated as follows:

E.E. = Total CUR - CUR in the supernatant/Total CUR *100

where the total of CUR was the initial amount of drug employed in the nanoparticle preparation and CUR in the SLN supernatant was determined by spectrophotometric analysis (UV–Vis, using a PerkinElmer Lambda Bio 20 spectrophotometer set at the wavelength of 425 nm). To assess the amount of CUR in the sample, a calibration curve in methanol was used in the concentration range $0.5 \cdot 10^{-3}$–0.01 mg/ml (R^2 = 0.999) [24,35]. Each measurement was performed in triplicate.

Loading Capacity (L.C.) for loaded SLN was calculated as follows:

L.C. = Total CUR - CUR in the supernatant /Total Gelucire®50/13 amount*100

Moreover, Entrapment Efficiency expressed as w/w for loaded SLN was calculated as follows:

w/w% = CUR entrapped/freeze dried SLN amount*100

2.4. Stability of SLN in simulated gastro-intestinal fluids

In view of *in vivo* studies, the physical stability of F2 and F4 was assessed by measuring their particle size after incubation in Simulated Gastric Fluid (SGF, pH 1.2) and Simulated Intestinal Fluid (SIF pH 6.8) or double distilled water containing 3% (w/w) of Tween®80 at 37 °C for 24 h. SGF was composed as follows: for 100 mL of final buffer, 0.7 mL of HCl (37%), 200 mg NaCl, 99.3 mL of H_2O. SIF was obtained by dissolving 680 mg KH_2PO_4 in the mixture of 92 mL of H_2O and 8 mL of a preformed solution of NaOH (0.2 N). Once formulated, F2 and F4 samples were subjected to centrifugation step, and diluted 1:7 (v/v) in SIF/Tween®80 (or double distilled water/Tween®80). The particle size was measured at different time intervals (0, 1, 2, 3, 5, 20 and 24 h) as described in Section 2.3.1. Each experiment was performed in triplicate
and results are expressed as mean ± standard deviation of each mean.

Furthermore, freshly prepared F2 samples were firstly freeze-dried for 72 h (T = −46 °C and P = 0.1 mBar, Lio Pascal 5P, Milan, Italy) and the resulting powders were evaluated for their stability upon storage at two different temperatures (*i.e.*, 20 °C and 4 °C) for three months by monitoring the CUR quantitative levels [36,37]. At different time points, appropriate aliquots of CUR-SLN were incubated in the presence of 1 mL of methanol at 37 °C for 30 min and, afterwards, the centrifugation was carried out as described in Section 2.2. The resulting supernatant was considered to retain CUR incorporated in the SLN and, thus, it was subjected to the spectrophotometric evaluation of CUR levels. Each assay was performed in triplicate.

2.5. In vitro release studies of CUR from SLN

To assess the capability of SLN to deliver *in vitro* the active agent CUR, release of CUR from F2 and F4 was carried out using dialysis bag [24]. The bag was filled with an amount ranging from 3 mg to 4 mg of CUR. Then, it was placed in a becker containing the release medium [*i.e.*, SGF or SIF] that was used each one after addition of 3% (w/w) of Tween®80 (final volume = 20 mL) in a thermostated bath set at 37 °C for 24 h under stirring. At predetermined time intervals 0.5 mL of the release medium were withdrawn and replaced with the same volume of fresh medium to maintain sink conditions. After centrifugation (16,000×*g*, 45 min, Eppendorf 5415D, Germany), in the supernatants the concentrations of the released CURC were determined by UV–Vis as described above. All release experiments were carried out in triplicate.

2.6. Cytotoxicity assay

To evaluate cell metabolic activity, Caco-2 were seeded in 96-well plates (10000 cells/cm^2) and treated with increasing doses (0.01, 0.1 and 0.2 mg/mL) of *N,O*-CMCS, CUR, F2 and F4. After 24 h of treatment, each sample was removed and cells were incubated with 3-(4,5-dimethylthiazol-2-yl)-2,5-diphenyltetrazolium bromide (MTT) solution (0.5 mg/mL). After 3 h, MTT solution was removed and sample was mixed with DMSO to assure the solubilization of formazan crystals. Optical density (OD) of DMSO solution was measured on Synergy HT at 570 nm and 670 nm (reference wavelength). Relative cell metabolic activity (%) was calculated as follows: 100×(ODs/ODc), where ODs represents the OD mean value of tested sample and ODc is the mean value of untreated cells (control). Each condition was tested in triplicate.

2.7. SLN uptake by Caco-2 cells

SLN uptake semi-quantitative analysis was performed as previously proposed, with some modifications [38]. Caco-2 cells were cultured in 96-well plates for 24 h at 37 °C, 5% CO_2. F2 and F4 formulations were added to well [0.2 mg/mL in culture medium without fetal bovine serum (FBS) and without phenol red] and incubated with cells for 15, 30, 120 and 360 min. At each considered incubation time, Caco-2 were washed with PBS and cellular uptake was evaluated, using a microplate reader (Synergy HT, BioTek, United Kingdom), equipped by an excitation filter at 485 nm and an emission filter at 528 nm. Data were expressed as fluorescence intensity, exploiting the auto-fluorescence property of CUR. As a control, cells were cultured and assessed in absence of samples. Each condition was performed in triplicate.

2.8. Transport studies through Caco-2 cells

To evaluate the transport capability of F2 and F4 through a Caco-2 cellular monolayer, these cells were seeded (4500 cells/cm^2) on permeable inserts (Corning HTS, Transwell®, 0.4μm pore size, 0.33 cm^2 growth area; Corning, Tewsbury, MA, USA). Experiment was carried out according to Sangsen et al. [39]. *Freeze dried* samples of F2 and F4 were suspended in DMEM-HG (without FBS and without phenol red) to obtain a final concentration of 0.2 mg/mL 100μL of each sample was added to the apical side of the insert, while 500μL of culture medium was added to basal side. Culture medium, without sample, was considered as negative control. After 15, 30, 120 and 360 min of incubation, the fluorescence intensity of both apical and basal medium was measured by Synergy HT (BioTek) (excitation filter at 485 nm, emission filter at 528 nm). Each condition was tested in duplicate. Results were expressed as fluorescence intensity mean values and standard deviations.

2.9. Anti-angiogenesis activity measured by d assay

The *in vivo* evaluation of anti-angiogenesis activity of the SLN was performed as follows. Fertilized White Leghorn chicken eggs (20 per group) were incubated at 37 °C at constant humidity. On day 3, a square window was opened in the shell, and, in order to detach the developing CAM from the shell, 2–3 mL of albumen were removed. The window was sealed with a glass, and the eggs were put again into the incubator. On day 8, eggs were treated with 1 mm^3 sterilized fragments of F1, F2, F3 and F4 formulations or a gelatin sponge soaked with 50 ng vascular endothelial growth factor (VEGF-A, R & D Systems, Abington, UK),

which was taken as a positive control, was placed on the top of the growing CAM, as previously described [40]. It should be noted that, in this assay, neither a negative control was inserted nor the number of blood vessels of untreated fertilized white egg was calculated because the inhibition e✓ect after the application of an external stimulus (*i.e.*, VEGF-A) was evaluated. CAMs were observed daily until day 12 and photographed *in ovo* with a stereomicroscope equipped with a camera system (Olympus Italia, Rozzano, Italy). At day 12, the angiogenic response was evaluated by the image analyzer system as the number of vessels converging the implant within the focal plane of the CAM. Means ± 1 Standard Deviation (SD) were evaluated for all the parameters and the statistical signi⌕cance of the di✓erences between the counts was calculated on 10 replicates for each treatment as below reported (Section 2.10).

2.10. Statistical analysis

Data of physicochemical characterization and stability of SLN formulations were statistically analyzed by one-way analysis of variance (ANOVA) and the Bonferroni's"post hoc"test for multiple comparison using GraphPad Prism v.4 software. Results of cytotoxicity assay, SLN uptake and transcellular transport study were processed by a multifactor ANOVA. MTT results were analyzed considering SLN formulations and concentrations as⌕xed factors while cell metabolic activity as dependent variable. For uptake and transport studies, incubation time and formulation are the⌕xed factors, while the dependent variable was the□uorescence intensity. The di✓erences between groups were analyzed with the post-hoc LSD's test for multiple comparisons. Data are expressed as mean ± standard deviation. The statistical signi⌕cance was⌕xed at $p < 0.05$. As for data related to the anti-angiogenic activity determined by CAM assay, Newman-Keuls multiple comparisons post-test was used to compare all treatment groups respect to the positive control after one-way ANOVA as well as to compare the e✓ect of a single treatment group respect to another one. The Graph Pad Prism 5.0 statistical package (GraphPad Software, San Diego, CA, USA) was used for these latter analyses and the limit for statistical signi⌕cance was set at $p < 0.05$.

3. Results

3.1. Physicochemical characterization of SLN

The main physicochemical properties of SLN prepared by the melt-emulsi⌕cation method with or without CUR are shown in Table 1. As seen, the CUR-unloaded SLN (F1) showed a particle size of 141 ± 11 nm, a value essentially comparable with those of the CUR-unloaded SLN decorated with *N,O*-CMCS (F3). On the other hand, it is noteworthy that the size of F4 SLN resulted about doubled in comparison with F3 SLN (649 ± 25 nm *vs* 366 ± 36 nm, respectively, Table 1). The PDI values of all SLN samples were in the range from 0.26 to 0.51 suggesting a quite broad particle size distribution [41]. The zeta potential of SLN control resulted of −9.7 ± 0.8 mV which decreased further in the presence of CUR (−21.3 ± 1.5 mV) or *N,O*-CMCS (−32.8 ± 1 mV). The most signi⌕cant decrease compared with the control ones was noted with the surface modi⌕ed and CUR-loaded SLN (*i.e.*, F4, -36.9 ± 1.8 mV, $p < 0.001$).

TEM analysis was used to assess the morphology of the nanoparticles prepared and, in such a way, their spherical shape as well as the absence of aggregated particles was proved (Fig. 1). Moreover, in Fig. 1a,b, a thick and lighter layer was observed around the particles of F3 evidencing the successful coating of *N,O*-CMCS on the surface of SLN. By comparing the size results from TEM with those from DLS it is clear that TEM evaluation returns a smaller particles for F3. It would be attributed to the hydration of the CMCS layer in aqueous suspension (DLS) while TEM analysis is performed at the dried state.

As expected on the basis of the high partition coe■cient of the CUR [log Po/w predicted 3.29, PubChem CID 969516; log P measured = 2.5 [42]], good values of E.E.% of the di✓erent SLN prepared were obtained (*i.e.*, of 65 ± 6 and 70 ± 4 for F2 and F4, respectively). Hence, there was not signi⌕cant di✓erence in E.E.% between the surface modi⌕ed and unmodi⌕ed SLN.

3.2. Solid state studies

To gain information on the solid state of SLN prepared, the corresponding FT-IR spectra and DSC thermograms were recorded and showed in Figs. 2 and 3, respectively. In particular, in Fig. 2 spectra of pure CUR, pure *N,O*-CMCS, F2 and F4 are reported. Characteristic peaks of pure CUR are the absorption bands at 3509 cm^{-1} and at 1628 cm^{-1} attributable to hydroxyl and unsatured C=O groups, respectively. The broad peak at 1622 cm^{-1} in the FT-IR spectrum of *N,O*-CMCS together with the absence of any absorption at 1730 cm^{-1} suggest that this carboxymethyl chitosan is in the –COONa form [43]. It was con⌕rmed also by comparing the FT-IR spectrum of *N,O*-CMCS in our hands with that reported for the sodium salt of *N,O*-CMCS [26]. The peaks at 3433 cm^{-1} and 1736 cm^{-1} observed in the FT-IR spectrum of CUR-SLN could be assigned to partially hydrated Gelucire®50/13 [44], while the stretching vibration at 1628 cm^{-1} is due to the presence of CUR. In the FT-IR spectrum of F4, both the band at 1628 cm^{-1} and the small absorption at 3509 cm^{-1} of CUR were noted together with the absorption band at 1736 cm^{-1}.

In Fig. 3, DSC thermograms of pure CUR, pure *N,O*-CMCS, pure Gelucire®50/13, F2 and F4 are reported. The thermogram of CUR revealed an endothermic peak at 178 °C corresponding to the melting of the drug [45]. The thermogram of pure *N,O*-CMCS showed a sharp endothermic peak at 150 °C which, following literature suggestions, should be due to water evaporation [43]. As shown in Fig. 3c, the DSC pro⌕le of pure Gelucire®50/13 exhibited a broad peak at 49 °C together

Table 1
Particle size, polydispersity index (PDI), zeta potential values, encapsulation e■ciency, loading capacity and entrapment e■ciency of di✓erent formulations pre-pared.[a]

Formulation (Code)	Size (nm)	PDI	Zeta Potential (mV)	Encapsulation E■ciency (E.E.%)	Loading Capacity (L.C.%)	Entrapment E■ciency (w/w%)
b-SLN (F1)	141 ± 11	0.28–0.40	−9.7 ± 0.8	–	–	–
CUR-SLN (F2)	366 ± 36**	0.26–0.41	−21.3 ± 1.5	65 ± 6	7.8 ± 0.7	45.0 ± 8.1
N,O-CMCS-*c*-SLN (F3)	131 ± 0.0	0.26–0.31	−32.8 ± 1.0	–	–	–
N,O-CMCS-*c*-CUR-SLN (F4)	649 ± 25**	0.42–0.51	−36.9 ± 1.8	70 ± 4	2.9 ± 0.4	70.4 ± 11.4

[a] Results are expressed as mean ± standard deviation (n = 6); **$p < 0.001$ for size is considered signi⌕cantly di✓erent compa

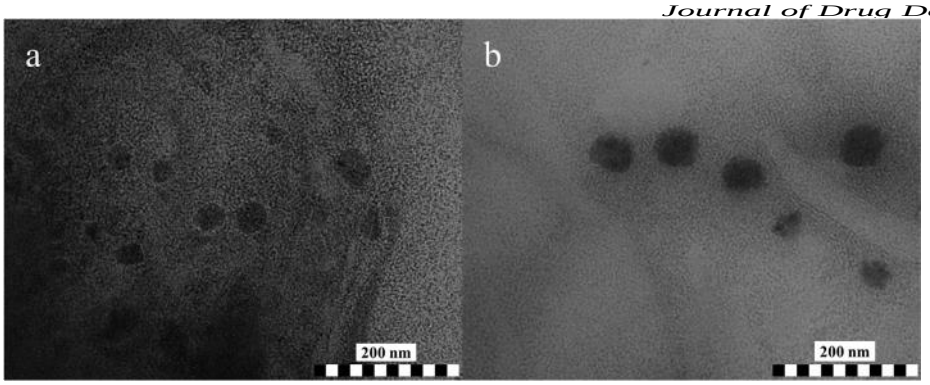

Fig. 1.TEM pictures of F3 (panels a,b). Scale bar 200 nm.

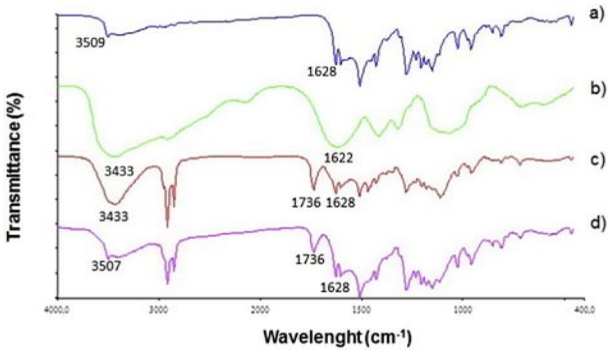

Fig. 2.FT-IR spectra of pure CUR (a), pure*N,O*-CMCS (b), F2 (c) and F4 (d).

with a small endothermic peak at 55 °C [32]. Noteworthy, both in the curve of F1 and F4, no peak neither at approximately 178 °C nor at 150 °C was observed. Moreover, even the characteristic peaks of Gelucire®50/13 were not detected in both the CUR-loaded SLN prepared.

3.3. Physical stability of surface-modi□ed and -unmodi□ed CUR-loaded SLN

The stability of F4 under gastro-intestinal conditions was investigated by monitoring the particle size after incubation in SGF and SIF containing 3% (w/w) of Tween®80 at 37 °C for 24 h. In SGF, such SLN samples formed large aggregated, while they resulted more stable after incubation in SIF and the corresponding results are shown in Fig. 4a. In this panel, for comparative purposes, the outcomes observed in double distilled water, are also reported. As shown, at the ⌕rst incubation times (2–3 h), an increase in particle size occurred both in SIF (*e.g.*, from 649 ± 25 to 806 ± 10) and double distilled water followed by a clear decrease in size and, after 5 h of incubation in SIF, the starting particle diameter was essentially maintained. Noteworthy, in double distilled water, at longer incubation times (more than 5 h) the particle size resulted even lower than at starting one. To evaluate the long-term stability of F2, the CUR content of these samples after storage at 4 °C and 20 °C up to 3 months was monitored and the relative results are shown in Fig. 4b. After 1 week of storage at 4 °C, the CUR content was essentially equal to the starting value. A slow decrease in the content of CUR was found after storage at 4 °C for two weeks (90% of the starting value), whereas prolonging storage at 3 months at 4 °C, the active principle content resulted in 62% of the starting value. Storage at 20 °C for 1 month led to a decrease in CUR content (80% of the starting value) which resulted of 60% of the starting value after storage at 20 °C for 3 months. It should be pointed out that only after three months of storage at 20 °C, visual inspection of F2 samples showed a yellow-brown colour indicative of chemical (oxidative and hydrolytic) degradation [20].

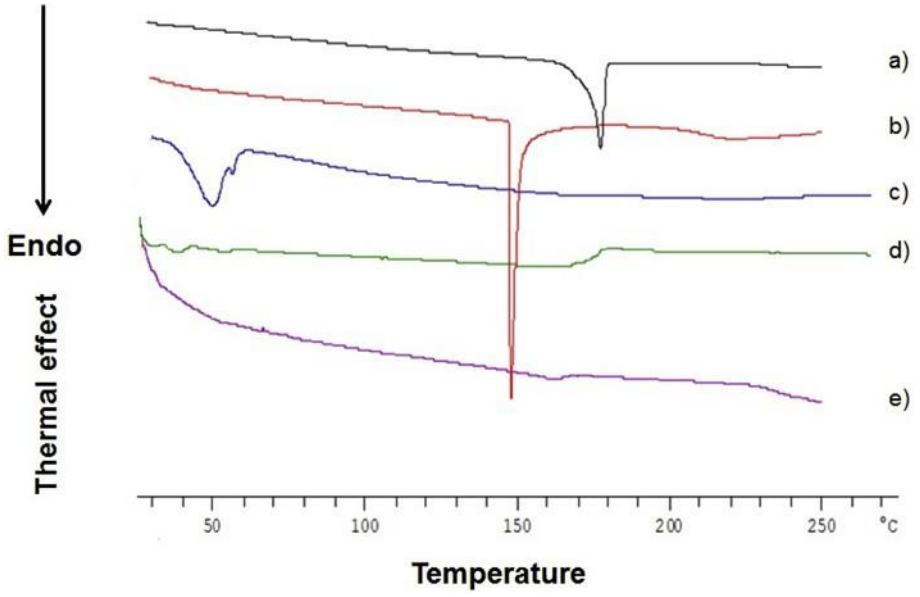

Fig. 3.DSC thermograms of pure CUR (a), pure*N,O*-CMCS (b), pure Gelucire®50/13 (c), F2 (d), and F4 (e).

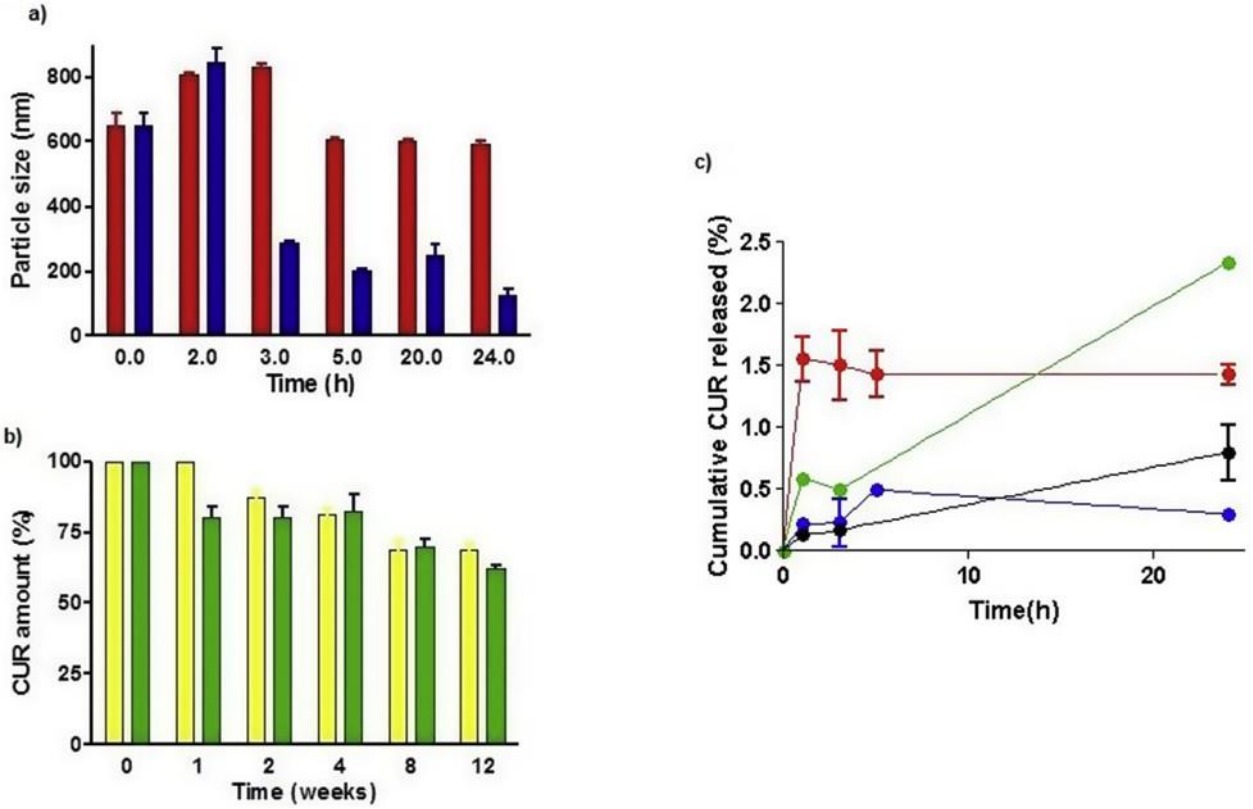

Fig. 4.a) Particle size changes of F4 incubated for 24 h at 37 °C. Red bars refer to incubation in SIF and blue bars refer to incubation in double distilled water; b) CUR content over the time after storage of F2 at 4 °C (yellow bars) and 20 °C (green bars); c) CUR released from F2 and F4 in SGF (blue and red curves, respectively) and in SIF (black and green curves, respectively). (For interpretation of the references to colour in this figure legend, the reader is referred to the Web version of this article.)

3.4. In vitro release studies

CUR release from F2 and F4 was studied up to 24 h using both SGF and SIF containing 3% (w/w) of Tween®80 as release medium (Fig. 4d). It was noted that, while F2 in SGF and in SIF showed negligible amounts of drug released, a greater CUR release occurred from F4 both in SGF and SIF, even though with a very different release profile. More precisely, F4 exhibited in SGF a burst drug release (red curve in Fig. 4d) whereas in SIF showed a sustained release (green curve in Fig. 4d) up to 24 h.

3.5. Cytotoxicity

The cytocompatibility of the proposed SLN was tested using Caco-2 cell line and considering three sample concentrations: 0.01, 0.1 and 0.2 mg/mL. These concentrations were already tested by us when CUR loaded polymeric micelles and nanoparticles [35,46] were previously studied. Moreover, these concentrations were selected also because they were suitable for detection of the entrapped CUR by spectrophotometric analysis as necessary for subsequent uptake study. Furthermore, we have also evaluated the Caco-2 viability after treatment with free*N,O*-CMCS and CUR and, particularly, the free drug was tested at the concentrations of 1.7, 17 and 34μg/mL which were equivalent to the CUR amounts loaded in SLN. Results demonstrated that both SLN formulations are cytocompatible at all considered concentrations, with a mean metabolic activity higher than 80% (Fig. 5). No significant differences ($p > 0.05$) were evidenced in terms of cell viability after the treatment with F2, F4, and*N,O*-CMCS. According to a cytotoxicity profile of CUR already shown elsewhere [35,47], cell incubation with free CUR significantly reduced the cell viability to 32–36%.

These results demonstrated that the proposed SLN were cytocompatible and, as already seen in previous works [21,46,48,49], the encapsulation of CUR in nanosystems seems to be a valid strategy to protect the cells from the cytotoxicity profile of the free CUR.

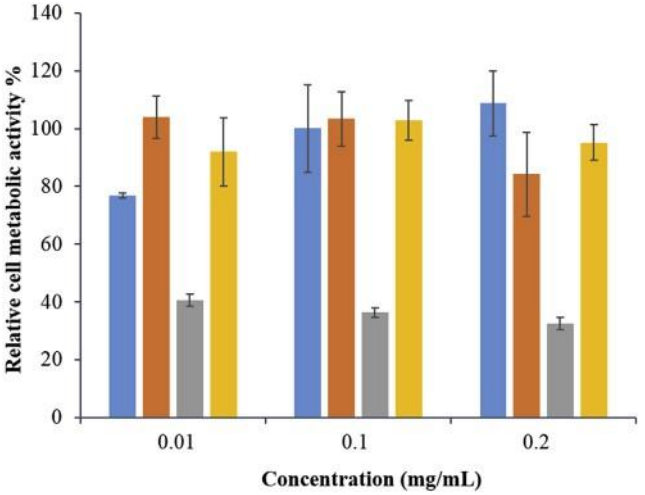

Fig. 5.Relative cell metabolic activity (percentage) of Caco-2 cells after 24 h treatment with different concentrations of F2 (orange bars), F4 (blue bars), freeCUR (grey bars) and*N,O*-CMCS (yellow bars). (For interpretation of the references to colour in this figure legend, the reader is referred to the Web version of this article.)

3.6. Uptake study

The ability of Caco-2 cells to uptake the proposed SLN was evaluated by a semi-quantitative analysis, exploiting the auto-fluorescence properties of CUR. Untreated and treated cells presented the same

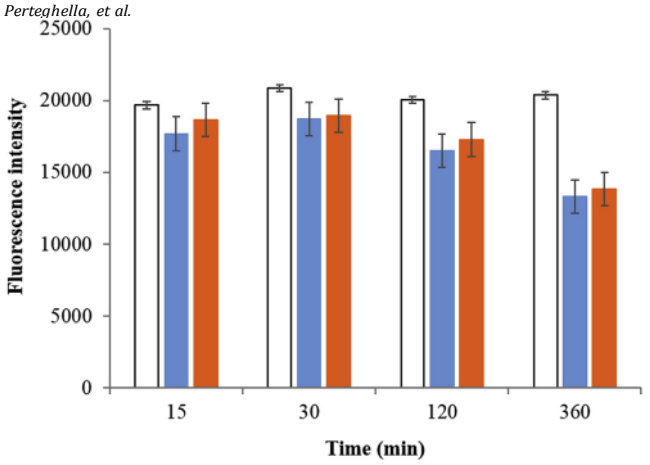

Fig. 6.SLN uptake by Caco-2 cells. Results are reported as mean values and standard deviations of uorescence intensity of Caco-2 incubated with sample for 15, 30, 120 and 360 min. Untreated cells (white bars); F2 (orange bars) and F4 (blue bars). (For interpretation of the references to colour in this gure legend, the reader is referred to the Web version of this article.)

uorescence intensity up to 120 min ($p > 0.05$). Fluorescence intensity of treated cells (blue and orange bars, Fig. 6) resulted reduced at 360 min, probably due to the cytotoxic e ect (and the consequent reduction of adherent cell number) exerted by the released CUR from SLN at such longer time point.

3.7. Caco-2 transcellular transport study

For the transcellular transport study, we seeded and cultured Caco-2 cells on Transwell plates for 28 days. After this time, the cells completely covered the culture insert and we added the samples in the apical side. After 15, 30, 120 and 360 min of incubation, we analyzed the uorescence intensity in basal sides. Results demonstrated that both F2 and F4 formulations were not able to cross the cellular monolayer (Fig. 7). Statistical analysis did not detect signi cant di erences between control and treatment groups ($p > 0.05$).

3.8. Anti-angiogenesis activity

The anti-angiogenic activity of F1–F4 was determined by the *in vivo* CAM assay. As shown in Fig. 8, all the SLN formulations, including the CUR-unloaded and surface unmodi ed F1, displayed statistically very signi cant anti-angiogenic activity compared with that showed by the

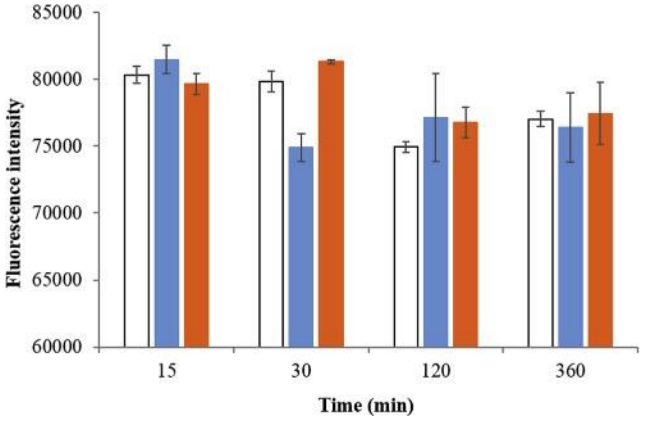

Fig. 7.Transport study of F2 and F4 on Caco-2 cells. Untreated cells (white bars); F2 (orange bars) and F4 (blue bars). (For interpretation of the references to colour in this gure legend, the reader is referred to the Web version of this article.)

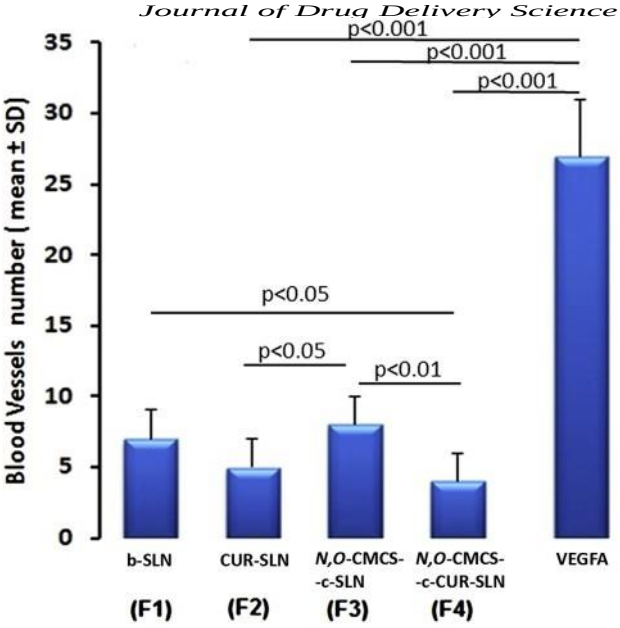

Fig. 8.Anti-angiogenic activity of F1–F4 formulations in the *in vivo* CAM assay. VEGF-A was used as positive control (pro-angiogenic). Each histogram shows the angiogenic response estimated as number of vessels converging toward the implant calculated on 10 replicates for each treatment (mean ± SD).

VEGF-A as positive control, as demonstrated by the low blood vessel number produced by each formulation. The CUR containing preparations F2 and F4 showed a higher anti-angiogenic activity than F1 and F3. Moreover, the di erences F1*vs*F4, F3*vs*F4, and F2*vs*F3 resultedstatistically signi cant, whereas for F1*vs*F2, F1*vs*F3 and F2*vs*F4 it was not observed. From these results it can be concluded that all the Gelucire®50/13 based SLN possessed signi cant anti-angiogenic properties, being the CUR containing and*N,O*-CMCS surface modi ed formulation F4 endowed with the highest anti-angiogenic activity.

4. Discussion

The purpose of this study was to evaluate the *in vivo* angiogenesis e ects of*N,O*-CMCS surface modi ed CUR-loaded SLN intended for oral administration of CUR which possesses multiple pharmacological activities including anti-angiogenic, anti-oxidant, anti-in ammatory and even anti-cancer e ects [50]. Therefore, some SLN formulations based on Gelucire®50/13 as lipid matrix (*i.e.*, F1–F4) were prepared and characterized.

It should be pointed out that previous studies evidenced that surface modi cation of SLN with chitosan and its derivatives such as*N*-CMCS or trimethyl chitosan greatly improves the oral delivery of lipophilic active principles with low chemical stability as CUR [20,27,51,52]. In general, the surface modi cation of SLN is successfully achieved exploiting the electrostatic interactions between the surface negative charge of SLN and the cationic charge properties of the surface modi er. However, such approach does not work well whether the surface modi er is constituted by a negatively charged polymer. This is the case of*N*-CMCS reported by Ref. [20] who prepared the corresponding*N*-CMCS coated CUR-loaded SLN starting from positively charged CUR-loaded SLN by adding stearylamine to the lipid phase. However, due to the risk of toxicity of cationic SLN [53], we ruled out this approach and chose to prepare the*N,O*-CMCS surface modi ed SLN by incubation of both CUR-loaded and CUR-unloaded SLN with a*N,O*-CMCS solution.

The successful surface modi cation of SLN with*N,O*-CMCS was proved by the increase of the particle size of CUR-loaded SLN (*i.e.*, 649 ± 25 nm, Table 1) as well as by the signi cant decrease of the zeta potential of these nanocarriers (*i.e.*,–36.9 ± 1.8 mV, Table 1), besides the visualization by TEM (Fig. 1). In a previous work, we suggested thatin SLN

consisting of Gelucire®50/13 a hydrophilic shell constituted of polyoxyethylene chains occurs together with an internal lipid layer he stearoyl moieties [31]. In such core-shell model, it maybe suggested that strong H-bonding interactions occur between the hydroxyl groups of*N,O*-CMCS and the oxygen atoms of the oxyethylene groups of the Gelucire®50/13 in the shell of nanocarrier. In addition, also strong hydrophobic interactions may occur between the ethylene moieties of the Gelucire®50/13 and the hydrophobic portion of the glucosamine nucleus of*N,O*-CMCS. Due to both these non-covalent interactions,*N,O*-CMCS may successfully be adsorbed on the surface of SLN.

The size increase of CUR-loaded SLN consequent to coating with the CS derivative is in agreement with that previously reported in literature [20]. The zeta potential reduction resulting from the*N,O*-CMCS coating should be due to the anionic properties of this polymer and it is confirmed by the corresponding FT-IR spectrum and DSC thermogram which proved that the*N,O*-CMCS used by us is in the–COONa form [26,43]. However, it is noteworthy the high PDI value (0.42–0.51) observed for F4 which mean that this nanoparticle formulation is not homogenous in size. In our opinion, this result could be related, at least in part, to the wide range of molecular weight (30–500 kDa) showed by the commercial*N,O*-CMCS used for coating. We believe that an appropriate selection and/or manufacturing method of this starting polymer should be beneficial to reduce the PDI value.

The solid state study based on FT-IR spectroscopy and thermal analysis (DSC) was performed in order to gain information on the internal structure of the encapsulated hydrophobic drug (CUR) in SLN. In this regard, it was evident that in the FT-IR spectra of F2 and F4 (Fig. 2c and d, respectively) the characteristic absorption bands of CUR (*i.e.,* 3509 cm^{-1} and 1728 cm^{-1}) were present while, in the corresponding thermograms of the same SLN, the distinctive endothermic peak at 178 °C, attributable to the melting of the drug, did not occur. This result could indicate that CUR is present in SLN in a non-crystalline state [54].

Despite several clinical applications of CUR, its therapeutic potential is limited mainly for its oxidative degradation and hydrolytic instability under physiological conditions. One of the advantages of SLN as drug carrier consists in the possible protection of the encapsulate drug against chemical degradation. It prompted us to assess the physical stability of CUR-loaded SLN prepared in this study measuring their particle size in simulated gastrointestinal fluids for 24 h as well as monitoring the CUR-content after storage for a long-term period (up to three months) at two different temperatures (*i.e.,*4 °C and 20 °C). As previously mentioned, under acidic conditions of SGF (pH 1.2), F4 formed large aggregated. Probably, such result may be ascribed to protonation of the carboxylate groups of*N,O*-CMCS leading to reduced aqueous solubility of this chitosan derivative. Conversely, under*quasi* neutral conditions of SIF (pH 6.8), no aggregation of F4 was noted and, after a transient increase in particle size, the starting particle diameter was essentially maintained. Interestingly, a similar behaviour was also showed by F4 in double distilled water where, at longer incubation times (more than 5 h), the particle size resulted even lower than that at the starting one. This last result may be accounted for taking into account that*N,O*-CMCS may be increasingly dissolved at pH > 5 with consequent reduction of the particle size. Hence, under SIF conditions as well as in double distilled water, these nanocarriers may be considered stable enough. It suggests that an aqueous suspension of F4 administered at prandial/post-prandial conditions [pH 5 of SGF [55] could be a promising strategy to overcome the drawback of aggregate formation in SGF pH 1.2. It is possible, indeed, that the less acidic environment of both water suspension of F4 and SGF pH 5, combined with the fast gastric empting of this liquid formulation may limit the particle aggregation observed in SGF pH 1.2, allowing appropriate delivery of CUR encapsulated at level of the small intestine, namely the main site of absorption for oral route. About the stability after storage for a long-term period of F2 the results showed that such lipid nanocarriers may be useful to protect CUR from oxidative and hydrolytic degradation for a long period at 4 °C, similarly to that found for other surface-modified SLN [20].

A further interesting result obtained in this work was the sustained release profile exhibited by F4 in SIF (pH 6.8), a feature required for appropriate delivery of CUR-loaded SLN for oral route, inhibiting so the burst release of CUR observed in SGF in acidic medium. Such results are also in agreement with those reported in literature for other surface-modified SLN [20]. However, it should be expected that release features should change dramatically*in vivo*where, due to the presence of lipases and other enzymes, the degradation of SLN should occur leading to a faster release of CUR.

It is noteworthy that both F2 and F4 formulations resulted cytocompatible with Caco-2 cells, while free CUR significantly reduced the cell viability to 32–36%. However, both F2 and F4 formulations were not able to*in vitro*pass through a Caco-2 cellular layer. As for the transport mechanism of F2 and F4 formulations it has been shown that SLN, as other nanoparticles, can be internalized by phagocytosis and pinocytosis mechanisms [56]. In particular, particles with a mean diameter higher than 500 nm tend to be internalized*via*phagocytosis while smaller particles (diameter lower than 200 nm) are mainly internalized by pinocytosis route [57]. Our nanosystems, showing mean diameters of about 400 and 700 nm (for F2 and F4, respectively) were supposed to undergo internalization by phagocytosis pathway, even though they resulted unable to cross the Caco-2 cellular monolayer. This phagocytosis pathway involves the particle recognition and then adhesion of the opsonized particles onto the cell membrane and finally ingestion by the cells [56]. A somewhat surprising was similar fluorescence intensity up to 120 min for untreated and treated cells observed in the uptake studies of F2 and F4 by Caco-2 cells because it is reported that surface modification with chitosan- or chitosan derivative of SLN could increase the oral bioavailability of CUR [52]. In this regard however, it should be considered that pitfalls may occur in*in vitro* uptake studies by fluorescence techniques and that notable divergences can be observed using confocal microscopy, flow cytometry and fluorescence spectroscopy methods, as recently highlighted by Seisel et al. [58]. In particular, these authors demonstrated, just using Caco-2 cells, that fluorescence intensity of a tracer may be substantially quenched by interactions dye/dye, dye/cellular lipids or dye/tryptophan residues of transmembrane cellular proteins [58]. On this basis, it is clear that the F2 and F4 uptake by Caco-2 cells cannot be surely checked by the semi-quantitiative analysis we used but*in vivo*studies are necessary before to draw definitive conclusions. Besides this, it should be taken into account that SLN may also be internalized by lymphatic circulation [20]. Moreover, as for the mechanisms underlying SLN cellular uptake, they are not fully understood, but it seems that some physicochemical features including particle size and surface charge as well as types of solid lipids and surface coating play an important role [27].

As for the interesting anti-angiogenesis effect showed by b-SLN (F1), it may be related to the presence of PEG-esters in the lipid matrix Gelucire®50/13 taking into account that the angiogenesis inhibition by PEGylated nanomicelles with core-shell geometry has already been observed [59,60]. The higher activity of CUR-containing formulations (F2 and F4) compared with the CUR-free ones (F1 and F3) should be due to the anti-angiogenesis properties of CUR. However, these results also evidenced the important role played by the*N,O*-CMCS coating in determining the anti-angiogenic activity of F3 and F4 which probably hinders the pro-angiogenic growth factor VEGF [29]. It still remains to be elucidated whether the anti-angiogenesis activity of F4 is due to a synergistic interaction between CUR/*N,O*-CMCS coating and the lipid matrix Gelucire®50/13.

5. Conclusions

In this work, CUR-loaded or unloaded SLN, as well as the corresponding*N,O*-CMCS surface modified SLN, were successfully prepared.

We have demonstrated the stability of F4 in intestinal fluid and sustained release of drug in the same medium. The stability tests after storage for a long-term period of F2 showed that such lipid nanocarriers may be useful to protect CUR from oxidative and hydrolytic degradation for a long period at 4 °C. Moreover, unlike free CUR, both F2 and F4 showed enhanced cytocompatibility with Caco-2 cells. Overall, results from the angiogenesis studies evidenced the interesting activity of the CUR-unloaded and surface unmodified F1 (*i.e.,* the b-SLN as such) as well as confirmed the hypothesis that *N,O*-CMCS decorating SLN gives anti-angiogenic features. Data also suggest that F4 may constitute an anti-angiogenic delivery platform for the potential oral administration of the CUR. Moreover, it appears that this delivery system is promising in vascular angiogenesis inhibition and may open the way for oral (co)-delivery of further anti-cancer drugs. However, *in vivo* studies are necessary to fully evaluate the therapeutic potential of F4 both for the oral delivery of CUR and for the possible role to target tumor vessels in "anti-tumor/anti-angiogenic" combined therapy.

CRediT authorship contribution statement

Sara Perteghella:Methodology, Investigation, Writing - review & editing.Delia Mandracchia:Methodology, Investigation.Maria Luisa Torre:Conceptualization, Writing - original draft.Roberto Tamma: Investigation, Software.Domenico Ribatti:Supervision, Writing - review & editing.Adriana Trapani:Conceptualization, Writing - original draft, Supervision.Giuseppe Tripodo:Methodology, Investigation, Writing - original draft.

Declaration of competing interest

None.

Acknowledgments

This work was partially financed by University of Bari (Italy) to A.T. (Cod. CUP:H91J11000160001). A.T., D.M and G.T. would like to acknowledge Dr. Claudio Perego (Gattefossè, Italy) for providing Gelucire®50/13 lipid.

Appendix A. Supplementary data

Supplementary data to this article can be found online at https://doi.org/10.1016/j.jddst.2019.101494.

References

[1] S. Talebian, J. Foroughi, S.J. Wade, K.L. Vine, A. Dolatshahi-Pirouz, M. Mehrali, J. Conde, G.G. Wallace, Biopolymers for antitumor implantable drug delivery systems: recent advances and future outlook, Adv. Mater. 30 (31) (2018).

[2] R.N. Gacche, R.J. Meshram, Angiogenic factors as potential drug target: efficacy and limitations of anti-angiogenic therapy, Biochim. Biophys. Acta Rev. Canc 1846 (1) (2014) 161–179.

[3] N.S. Vasudev, A.R. Reynolds, Anti-angiogenic therapy for cancer: current progress, unresolved questions and future directions, Angiogenesis 17 (3) (2014) 471–494.

[4] J. Folkman, Anti-angiogenesis: new concept for therapy of solid tumors, Ann. Surg. 175 (3) (1972) 409–416.

[5] D. Banerjee, R. Harfouche, S. Sengupta, Nanotechnology-mediated targeting of tumor angiogenesis, Vasc. Cell 3 (1) (2011).

[6] M.L. Bondi, C. Botto, E. Amore, M.R. Emma, G. Augello, E.F. Craparo, M. Cervello, Lipid nanocarriers containing sorafenib inhibit colonies formation in human hepatocarcinoma cells, Int. J. Pharm. 493 (1–2) (2015) 75–85.

[7] J.H. Duan, H.M. Mansour, Y.D. Zhang, X.M. Deng, Y.X. Chen, J.W. Wang, Y.F. Pan, J.F. Zhao, Reversion of multidrug resistance by co-encapsulation of doxorubicin and curcumin in chitosan/poly(butyl cyanoacrylate) nanoparticles, Int. J. Pharm. 426 (1–2) (2012) 193–201.

[8] Q.F. Guo, X.L. Li, Y. Yang, J. Wei, Q. Zhao, F. Luo, Z.Y. Qian, Enhanced 4T1 breast carcinoma anticancer activity by Co-delivery of doxorubicin and curcumin with core-shell drug-carrier based on heparin modified poly(L-lactide) grafted polyethylenimine cationic nanoparticles, J. Biomed. Nanotechnol. 10 (2) (2014) 227–237.

[9] J.M. Zhang, J.J. Li, Z. Shi, Y. Yang, X. Xie, S.M. Lee, Y.T. Wang, K.W. Leong, M.W. Chen, pH-sensitive polymeric nanoparticles for co-delivery of doxorubicin and curcumin to treat cancer via enhanced pro-apoptotic and anti-angiogenic activities, Acta Biomater. 58 (2017) 349–364.

[10] Y.X. Dai, S. Wang, W.B. Shi, M.D. Lang, pH-responsive carboxymethyl chitosan-derived micelles as apatinib carriers for effective anti-angiogenesis activity: preparation and in vitro evaluation, Carbohydr. Polym. 176 (2017) 107–116.

[11] N. Nasongkla, X. Shuai, H. Ai, B.D. Weinberg, J. Pink, D.A. Boothman, J.M. Gao, cRGD-functionalized polymer micelles for targeted doxorubicin delivery, Angew. Chem. Int. Ed. 43 (46) (2004) 6323–6327.

[12] X.L. Xu, L. Li, Z. Zhou, W. Sun, Y. Huang, Dual-pH responsive micelle platform for co-delivery of axitinib and doxorubicin, Int. J. Pharm. 507 (1–2) (2016) 50–60.

[13] S.T. Guo, L. Huang, Nanoparticles containing insoluble drug for cancer therapy, Biotechnol. Adv. 32 (4) (2014) 778–788.

[14] H.L. Wong, R. Bendayan, A.M. Rauth, Y.Q. Li, X.Y. Wu, Chemotherapy with anticancer drugs encapsulated in solid lipid nanoparticles, Adv. Drug Deliv. Rev. 59 (6) (2007) 491–504.

[15] N. Matougui, L. Boge, A.C. Groo, A. Umerska, L. Ringstad, H. Bysell, P. Saulnier, Lipid-based nanoformulations for peptide delivery, Int. J. Pharm. 502 (2016) 80–97.

[16] G. Trapani, M. Franco, A. Trapani, A. Lopedota, A. Latrofa, E. Gallucci, S. Micelli, G. Liso, Frog intestinal sac: a new in vitro method for the assessment of intestinal permeability, J. Pharmaceut. Sci. 93 (12) (2004) 2909–2919.

[17] M. Uner, G. Yener, Importance of solid lipid nanoparticles (SLN) in various administration routes and future perspectives, Int. J. Nanomed. 2 (3) (2007) 289–300.

[18] G. K Kaur, M. Arora, R.K. Majeti, Oral drug delivery technologies-a decade of developments, J. Pharmacol. Exp. Therapeut. (2019) 529–543.

[19] L. Battaglia, M. Gallarate, E. Peira, D. Chirio, I. Solazzi, S.M.A. Giordano, C.L. Gigliotti, C. Riganti, C. Dianzani, Bevacizumab loaded solid lipid nanoparticles prepared by the coacervation technique: preliminary in vitro studies, Nanotechnology 26 (25) (2015).

[20] J.S. Baek, C.W. Cho, Surface modification of solid lipid nanoparticles for oral delivery of curcumin: improvement of bioavailability through enhanced cellular uptake, and lymphatic uptake, Eur. J. Pharm. Biopharm. 117 (2017) 132–140.

[21] G. Tripodo, G. Pasut, A. Trapani, A. Mero, F.M. Lasorsa, T. Chlapanidas, G. Trapani, D. Mandracchia, Inulin-D-α-tocopherol succinate (INVITE) nanomicelles as a platform for effective intravenous administration of curcumin, Biomacromolecules 16 (2015) 550–557.

[22] A. Trapani, V. Laquintana, A. Lopedota, M. Franco, A. Latrofa, G. Talani, E. Sanna, G. Trapani, G. Liso, Evaluation of new propofol aqueous solutions for intravenous anesthesia, Int. J. Pharm. 278 (1) (2004) 91–98.

[23] Vivek R. Yadav, Sarasija Suresh, Kshama Devi, Seema Yadav, Effect of cyclodextrin complexation of curcumin on its solubility and antiangiogenic and anti-inflammatory activity in rat colitis model, AAPS PharmSciTech 10 (3) (2009) 752–762.

[24] D. Mandracchia, G. Tripodo, A. Trapani, S. Ruggieri, T. Annese, T. Chlapanidas, G. Trapani, D. Ribatti, Inulin based micelles loaded with curcumin or celecoxib with effective anti-angiogenic activity, Eur. J. Pharmaceut. Sci. 93 (2016) 141–146.

[25] J.M. Zhang, J.J. Li, Z. Shi, Y. Yang, X. Xie, S.M. Lee, Y.T. Wang, K.W. Leong, M.W. Chen, pH-sensitive polymeric nanoparticles for co-delivery of doxorubicin and curcumin to treat cancer via enhanced pro-apoptotic and anti-angiogenic activities, Acta Biomater. 58 (2017) 349–364.

[26] Z.W. Jiang, B.Q. Han, H. Li, Y. Yang, W.S. Liu, Carboxymethyl chitosan represses tumor angiogenesis in vitro and in vivo, Carbohydr. Polym. 129 (2015) 1–8.

[27] Y.C. Luo, Z. Teng, Y. Li, Q. Wang, Solid lipid nanoparticles for oral drug delivery: chitosan coating improves stability, controlled delivery, mucoadhesion and cellular uptake, Carbohydr. Polym. 122 (2015) 221–229.

[28] N.N. Ferreira, L.M.B. Ferreira, V. Miranda-Goncalves, R.M. Reis, T.V. Seraphim, J.C. Borges, F. Baltazar, M.P.D. Gremiao, Alginate hydrogel improves anti-angiogenic bevacizumab activity in cancer therapy, Eur. J. Pharm. Biopharm. 119 (2017) 271–282.

[29] G. Tripodo, A. Trapani, A. Rosato, C. Di Franco, R. Tamma, G. Trapani, D. Ribatti, D. Mandracchia, Hydrogels for biomedical applications from glycol chitosan and PEG diglycidyl ether exhibit pro-angiogenic and antibacterial activity, Carbohydr. Polym. 198 (2018) 124–130.

[30] A. Trapani, D. Mandracchia, C. Di Franco, H. Cordero, P. Morcillo, R. Cornparelli, A. Cuesta, M.A. Esteban, In vitro characterization of 6-Coumarin loaded solid lipid nanoparticles and their uptake by immunocompetent fish cells, Colloids Surf. B Biointerfaces 127 (2015) 79–88.

[31] A. Trapani, G. Tripodo, D. Mandracchia, N. Cioff, N. Ditaranto, V. De Leo, H. Cordero, M.A. Esteban, Glutathione-loaded solid lipid nanoparticles based on Gelucire (R) 50/13: spectroscopic characterization and interactions with fish cells, J. Drug Deliv. Sci. Technol. 47 (2018) 359–366.

[32] S. Castellani, A. Trapani, A. Spagnoletta, L. di Toma, T. Magrone, S. Di Gioia, D. Mandracchia, G. Trapani, E. Jirillo, M. Conese, Nanoparticle delivery of grape seed-derived proanthocyanidins to airway epithelial cells dampens oxidative stress and inflammation, J. Transl. Med. 16 (2018).

[33] A. Trapani, C. Palazzo, M. Contino, M.G. Perrone, N. Cioff, N. Ditaranto, N.A. Colabufo, M. Conese, G. Trapani, G. Puglisi, Mucoadhesive properties and interaction with P-glycoprotein (P-gp) of thiolated-chitosans and -glycol chitosans and corresponding parent polymers: a comparative study, Biomacromolecules 15 (3) (2014) 882–893.

[34] A. Aresta, C.D. Calvano, A. Trapani, S. Cellamare, C.G. Zambonin, E. De Giglio, Development and analytical characterization of vitamin(s)-loaded chitosan nanoparticles for potential food packaging applications, J. Nanoparticle Res. 15 (4) (2013).

[35] G. Tripodo, T. Chlapanidas, S. Perteghella, B. Vigani, D. Mandracchia, A. Trapani,

M. Galuzzi, M.C. Tosca, B. Antonioli, P. Gaetani, M. Marazzi, M.L. Torre, Mesenchymal stromal cells loading curcumin-INVITE-micelles: a drug delivery system for neurodegenerative diseases, Colloids Surf. B Biointerfaces 125 (2015) 300–308.
[36] A. Trapani, D. Mandracchia, G. Tripodo, S. Cometa, S. Cellamare, E. De Giglio, P. Klepetsanis, S.G. Antimisiaris, Protection of dopamine towards autoxidation reaction by encapsulation into non-coated- or chitosan- or thiolated chitosan-coated-liposomes, Colloids Surf. B Biointerfaces 170 (2018) 11–19.
[37] A. Trapani, D. Tricarico, A. Mele, F. Maqoud, D. Mandracchia, P. Vitale, V. Capriati, G. Trapani, V. Dimiccolil, A. Tolomeol, A. Scilimati, A novel injectable formulation of 6-□uoro-(L)-DOPA imaging agent for diagnosis of neuroendocrine tumors and Parkinson's disease, Int. J. Pharm. 519 (1–2) (2017) 304–313.
[38] J. Kundu, Y.I. Chung, Y.H. Kim, G. Taeb, S.C. Kundu, Silk⌕broin nanoparticles for cellular uptake and control release, Int. J. Pharm. 388 (1–2) (2010) 242–250.
[39] Y. Sangsen, K. Wiwattanawongsa, K. Likhitwitayawuid, B. Sritularak, P. Graidist, R. Wiwattanapatapee, In□uence of surfactants in self-microemulsifying formulations on enhancing oral bioavailability of oxyresveratrol: studies in Caco-2 cells and in vivo, Int. J. Pharm. 498 (1–2) (2016) 294–303.
[40] D. Ribatti, B. Nico, A. Vacca, M. Presta, The gelatin sponge-chorioallantoic membrane assay, Nat. Protoc. 1 (1) (2006) 85–91.
[41] M. Gaumet, A. Vargas, R. Gurny, F. Delie, Nanoparticles for drug delivery: the need for precision in reporting particle size parameters, Eur. J. Pharm. Biopharm. 69 (1) (2008) 1–9.
[42] S. Fujisawa, T. Atsumi, M. Ishihara, Y. Kadoma, Cytotoxicity, ROS-generation activity and radical-scavenging activity of curcumin and related compounds, Anticancer Res. 24 (2B) (2004) 563–569.
[43] V.K. Mourya, N.N. Inamdar, A. Tiwari, Carboxymethyl chitosan and its applications, Adv. Mater. Lett. 1 (1) (2010) 22.
[44] M. El Hadri, A. Achahbar, J. El Khamkhami, B. Khelifa, V. Faivre, O. Abbas, S. Bresson, Lyotropic behavior of Gelucire 50/13 by XRD, Raman and IR spectroscopies according to hydration, Chem. Phys. Lipids 200 (2016) 11–23.
[45] Y.K. Huang, L. Hu, S. Huang, W.J. Xu, J.Y. Wan, D.D. Wang, G.C. Zheng, Z.N. Xia, Curcumin-loaded galactosylated BSA nanoparticles as targeted drug delivery carriers inhibit hepatocellular carcinoma cell proliferation and migration, Int. J. Nanomed. 13 (2018) 8309–8323.
[46] B. Crivelli, E. Bari, S. Perteghella, L. Catenacci, M. Sorrenti, M. Mocchi, S. Farago, G. Tripodo, A. Prina-Mello, M.L. Torre, Silk⌕broin nanoparticles for celecoxib and curcumin delivery: ROS-scavenging and anti-in□ammatory activities in an in vitro model of osteoarthritis, Eur. J. Pharm. Biopharm. 137 (2019) 37–45.
[47] Z.L. Kong, H.P. Kuo, A. Johnson, L.C. Wu, K.L.B. Chang, Curcumin-Loaded mesoporous silica nanoparticles markedly enhanced cytotoxicity in hepatocellular carcinoma cells, Int. J. Mol. Sci. 20 (12) (2019).
[48] S. Perteghella, B. Crivelli, L. Catenacci, M. Sorrenti, G. Bruni, V. Necchi, B. Vigani, M. Sorlini, M.L. Torre, T. Chlapanidas, Stem cell-extracellular vesicles as drug delivery systems: new frontiers for silk/curcumin nanoparticles, Int. J. Pharm. 520 (1–2) (2017) 86–97.
[49] B. Crivelli, S. Perteghella, E. Bari, M. Sorrenti, G. Tripodo, T. Chlapanidas, M.L. Torre, Silk nanoparticles: from inert supports to bioactive natural carriers for drug delivery, Soft Matter 14 (4) (2018) 546–557.
[50] R.K. Maheshwari, A.K. Singh, J. Gaddipati, R.C. Srimal, Multiple biological activities of curcumin: a short review, Life Sci. 78 (18) (2006) 2081–2087.
[51] P. Ramalingam, Y.T. Ko, Improved oral delivery of resveratrol from N-trimethyl chitosan-g-palmitic acid surface-modi⌕ed solid lipid nanoparticles, Colloids Surf. B Biointerfaces 139 (2016) 52–61.
[52] P. Ganesan, P. Ramalingam, G. Karthivashan, Y.T. Ko, D.K. Choi, Recent developments in solid lipid nanoparticle and surface-modi⌕ed solid lipid nanoparticle delivery systems for oral delivery of phyto-bioactive compounds in various chronic diseases, Int. J. Nanomed. 13 (2018) 1569–1583.
[53] R. Cortesi, M. Campioni, L. Ravani, M. Drechsler, M. Pinotti, E. Esposito, Cationic lipid nanosystems as carriers for nucleic acids, N. Biotech. 31 (1) (2014) 44–54.
[54] A. Gumireddy, R. Christman, D. Kumari, A. Tiwari, E.J. North, H. Chauhan, Preparation, characterization, and in vitro evaluation of curcumin- and resveratrol-loaded solid lipid nanoparticles, AAPS PharmSciTech 20 (4) (2019).
[55] A.P. Ault, D.I. Stark, J.L. Axson, J.N. Keeney, A.D. Maynard, I.L. Bergin, M.A. Philbert, Protein corona-induced modi⌕cation of silver nanoparticle aggregation in simulated gastric□uid, Environ. Sci. Nano 3 (6) (2016) 1510–1520 .
[56] S. Martins, S. Costa-Lima, T. Carneiro, A. Cordeiro-da-Silva, E.B. Souto, D.C. Ferreira, Solid lipid nanoparticles as intracellular drug transporters: an investigation of the uptake mechanism and pathway, Int. J. Pharm. 430 (1–2) (2012) 216–227.
[57] H.J. Je, E.S. Kim, J.S. Lee, H.G. Lee, Release properties and cellular uptake in Caco-2 cells of size-controlled chitosan nanoparticles, J. Agric. Food Chem. 65 (50) (2017) 10899–10906.
[58] P. Seisel, F. Pelletier, S. Deshayes, P. Boisguerin, How to evaluate the cellular uptake of CCPs with□uorescence techniques: dissecting methodological pitfalls associated to tryptophan-rich peptides, Biochim. Biophys. Acta Biomembr. 1861 (9) (2019) 13.
[59] Y.K. Li, Y.Y. Wu, L. Huang, L. Miao, J.P. Zhou, A.B. Satterlee, J. Yao, Sigma receptor-mediated targeted delivery of anti-angiogenic multifunctional nanodrugs for combination tumor therapy, J. Contr. Release 228 (2016) 107–119.
[60] T. Zhou, Q.L. Dong, Y. Shen, W. Wu, H.D. Wu, X.L. Luo, X.L. Liao, G.X. Wang, PEG-b-PCL polymeric nano-micelle inhibits vascular angiogenesis by activating p53-dependent apoptosis in zebra⌕sh, Int. J. Nanomed. 11 (2016) 6517–6531 .